The Astrophysical Journal, 605:L77–L80, 2004 April 10

DOWNFLOW MOTIONS ASSOCIATED WITH IMPULSIVE NONTHERMAL EMISSIONS OBSERVED IN THE 2002 JULY 23 SOLAR FLARE

Ayumi Asai,[1,2] Takaaki Yokoyama,[3] Masumi Shimojo,[4] and Kazunari Shibata[1]
Received 2003 December 23; accepted 2004 March 1; published 2004 March 11

ABSTRACT

We present a detailed examination of downflow motions above flare loops observed in the 2002 July 23 flare. The extreme-ultraviolet images obtained with the *Transition Region and Coronal Explorer* show dark downflow motions (sunward motions) above the postflare loops, not only in the decay phase but also in the impulsive and main phases. We also found that the times when the downflow motions start to be seen correspond to the times when bursts of nonthermal emissions in hard X-rays and microwaves are emitted. This result implies that the downflow motions occurred when strong magnetic energy was released and that they are, or are correlated with, reconnection outflows.

Subject headings: Sun: activity — Sun: chromosphere — Sun: corona — Sun: flares — Sun: X-rays, gamma rays

1. INTRODUCTION

The finding of supra-arcade downflow motions (downflows) is one of the most important results that the soft X-ray telescope (SXT; Tsuneta et al. 1991) aboard *Yohkoh* (Ogawara et al. 1991) achieved. McKenzie & Hudson (1999) and McKenzie (2000) examined, in detail, these dark and sometimes bright features moving sunward from the high corona with speeds of 45–500 km s^{-1}. They also performed the temperature analysis with the filter ratio method (Hara et al. 1992), although it is very difficult to extract these physical values for such low emission features owing to instrumental effects like scattering. They reported that the density and temperature of the downflows are about 10^9 cm^{-3} and 10^7 K, respectively. Although these values contain considerable uncertainties, they suggested that they are "moving voids," which consist of such low-density and high-temperature plasma. These voids are pushed downward because of magnetic reconnection that occurred at higher altitudes, and therefore, they are thought to be new observational and morphological evidence of magnetic reconnection. Moreover, downflows are seen only in superhot plasma regions, which are located within cusp structures above postflare loops (Akiyama 2001; Tsuneta 1996). The regions are also located beneath the reconnection points and are defined by magnetic flux that has just gone through reconnection. Therefore, the regions can be used to obtain some direct information about the magnetic reconnection process.

Recently, Innes, McKenzie, & Wang (2003a, 2003b) reported similar downflows in extreme-ultraviolet (EUV) images obtained with the *Transition Region and Coronal Explorer* (*TRACE*; Handy et al. 1999; Schrijver et al. 1999) and the Solar Ultraviolet Measurements of Emitted Radiation (SUMER) instrument (Wilhelm et al. 1995) aboard the *Solar and Heliospheric Observatory* (*SOHO*; Domingo, Fleck, & Poland 1995). By using the *TRACE* images, we have been able to examine downflows with higher spatial resolution than was done with *Yohkoh*/SXT. Furthermore, the SUMER data give spectroscopic information about the downflow. The results of spectroscopic analyses, which Innes et al. (2003a) performed, discard the possibility that the downflows are cold absorbing material and support a model in which the downflows are moving voids. Innes et al. (2003b) found that highly blueshifted features, which correspond to a Doppler velocity of up to 1000 km s^{-1}, were associated with the downflows, although it was not clear if they were the reconnection outflows themselves.

In this Letter, we examine the relationship between downflows and hard X-ray (HXR) emission, which implies strong energy release. If downflows are really related to magnetic reconnection, they are expected to be observed even in the impulsive phase, when magnetic reconnection occurs vigorously, and when nonthermal emissions are observed in HXRs and in microwaves. So far, almost all the downflows have been observed in long-duration event (LDE) flares, and many of them (about 70% of all) were observed after the peak times of soft X-ray (SXR) light curves (McKenzie & Hudson 2001; Hudson & McKenzie 2001). In these events, therefore, HXR enhancements are not so strong to be compared with downflows. Moreover, although the *TRACE* downflows that Innes et al. (2003a, 2003b) examined were observed to be accompanied by the impulsive HXR emission in the rise phase of an LDE flare, we could hardly identify the relationship between the downflows and the HXR emissions. This is because the size of the flare structure was huge, and too many downflows were observed at a time. On the other hand, in the 2002 July 23 solar flare we observed the *TRACE* downflows and the impulsive HXR bursts simultaneously. Furthermore, we revealed, for the first time, that each downflow is correlated with HXR emission, since we could see few downflows at a time. In § 2, we summarize the observational data and the features of the flare. In § 3, we examine the downflows. We investigate the times when the downflows are seen and compare them with the nonthermal radiation in HXRs and microwaves. In § 4, a summary and discussion are given.

2. OBSERVATIONS

A large solar flare (X4.8 on the *GOES* scale) occurred in NOAA Active Region 10039 (S12°, E72°) at 00:18 UT, 2002 July 23. It showed a lot of spectacular features, which have been reported in a number of papers (e.g., Lin et al. 2003), and is famous as the first event in which γ-ray images were successfully obtained (Hurford et al. 2003) with the *Reuven*

[1] Kwasan and Hida Observatories, Kyoto University, Yamashina-ku, Kyoto 607-8471, Japan; asai@kwasan.kyoto-u.ac.jp.
[2] Research Fellows of the Japan Society for the Promotion of Science.
[3] Department of Earth and Planetary Science, University of Tokyo, Hongo, Bunkyo, Tokyo 113-0033, Japan.
[4] Nobeyama Radio Observatory, Minamisaku, Nagano, 384-1305, Japan.

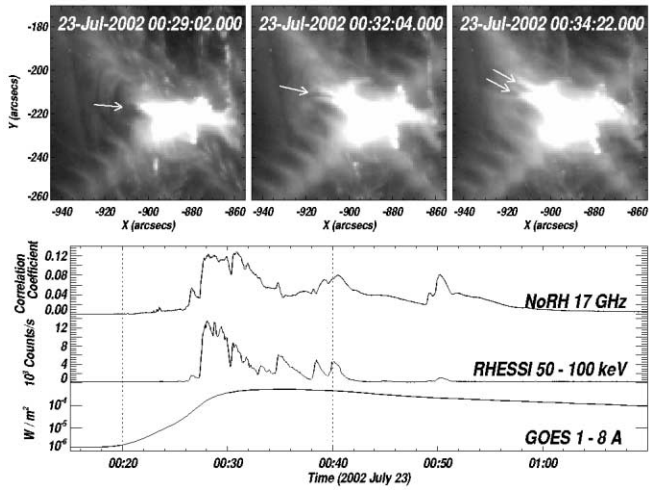

FIG. 1.—*Top*: Temporal evolution of the 2002 July 23 flare in EUV 195 Å obtained with *TRACE*. Solar north is up, and west is to the right. The horizontal and vertical axes give the distance from the disk center in units of arcseconds. The white arrows indicate the downflows. The cross-shaped fringe structure is due to diffraction. *Bottom*: Light curves of the 2002 July 23 flare. *From top to bottom*: Radio correlation plot observed at 17 GHz with NoRH, HXR count rate measured with *RHESSI* (50–100 keV), and SXR flux in the *GOES* 1.0–8.0 Å channel. The two dotted vertical lines show the time range of the time slice images in Fig. 2.

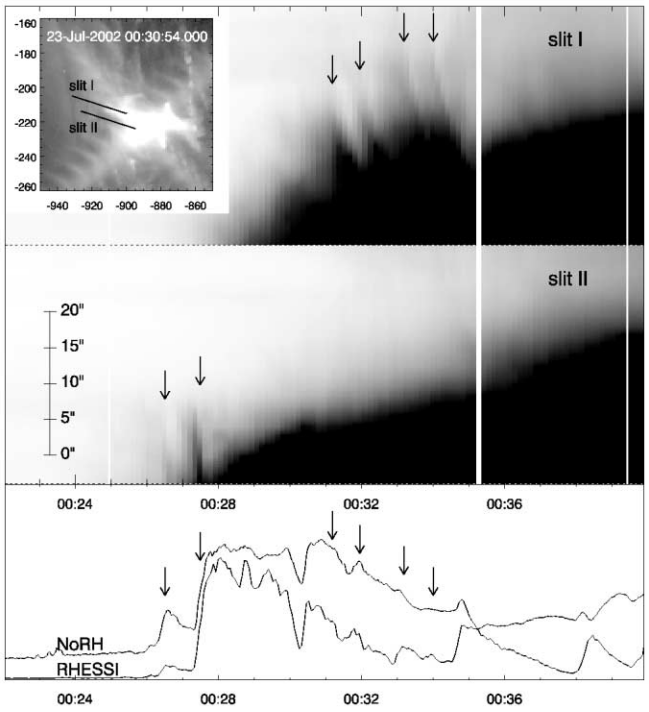

FIG. 2.—*Top left*: EUV image of the flare obtained with *TRACE*. The black solid lines illustrate the position of the slit lines I and II. *Top right and middle*: Time-sequenced EUV (195 Å) images obtained with *TRACE* along the slit lines I and II, respectively. The horizontal axis is time (UT), and the vertical axis is the space along the slits. *Bottom*: Microwave (17 GHz) and HXR (50–100 keV) light curves obtained with NoRH and *RHESSI*, respectively.

Ramaty High Energy Solar Spectroscopic Imager (*RHESSI*; Lin et al. 2002). Moreover, the vertical evolution, such as ejections, formation of postflare loops, downflows, and so on, are clearly seen, since the flare site is located near the southeast limb.

EUV images of the flare were obtained with *TRACE*. We used 195 Å images, in which the Fe XII line formed at ~1 MK is dominant. An emission line of Fe XXIV, formed at ~20 MK, is also contained but is usually much weaker (Handy et al. 1999). The pixel size of the CCD is 1.″0, and the temporal resolution is about 9 s. The top panels of Figure 1 show the temporal evolution of the flare in the EUV. We cannot see clearly the postflare loops owing to saturation of the images, but we can see a cross-shaped fringe pattern, like fish bones, due to diffraction. Although the superhot plasma region is much fainter than the postflare loops, it is visibly spread above the loops. Krucker, Hurford, & Lin (2003) performed the co-alignment between the HXR data of the flare obtained with *RHESSI* and the EUV image with *TRACE* and reported that the HXR coronal source is seen in the *RHESSI* low-energy range, 12–18 keV, and is located on the superhot plasma region seen in the *TRACE* 195 Å images. Emslie et al. (2003) performed imaging spectroscopy of the source and reported that the region consists of thermal plasma, which has a high temperature of up to 40 MK.

To examine nonthermal electrons, we also used the microwave total flux measured with the Nobeyama Radioheliograph (NoRH; Nakajima et al. 1994) and HXR data taken with *RHESSI*. The bottom panel of Figure 1 shows the light curves of the flare in microwaves, HXRs, and SXRs. The top line is that of NoRH, 17 GHz, the middle one is that of *RHESSI*, 50–100 keV, and the bottom one is that of the *GOES* 1.0–8.0 Å channel. As White et al. (2003) reported, the light curve in microwaves is quite similar to that in the HXR high-energy range (greater than 50 keV).

3. TRACE DOWNFLOWS

In the 2002 July 23 flare, we can see some dark downflows above the postflare loops between about 00:26 and 01:20 UT. This time range corresponds not only to the decay phase but also to the impulsive and main phases of the flare (see the light curves of Fig. 1). Here we concentrate on the vertical motion and the timing of the downflows. The top right and middle panels in Figure 2 show time slice images from 00:20 to 00:40 UT (negative images). This time range of the time slice images corresponds to the impulsive phase, and the chosen area is the sandwiched duration with two vertical dotted lines in the bottom panel of Figure 1. The bottom dark (bright in the real images) regions are postflare loops. They are so bright in the *TRACE* images because of saturation that no fine structure is identified. Above this region, we can see a much fainter dark region—the superhot region. Several downflows can be seen, which are pointed out with arrows. The apparent speeds of the downflows are between 100 and 250 km s^{-1}. They are decelerated at the top of the postflare loops. The bottom panel in Figure 2 shows the HXR and microwave light curves obtained with *RHESSI* (50–100 keV) and NoRH (17 GHz), respectively. The arrows point out the same times shown in the upper panels. They correspond to the times when nonthermal bursts occur. The HXR and microwave intensities are thought to be proportional to the amount of the magnetic energy released per unit time (Neupert 1968; Wu et al. 1986; Hudson 1991). Therefore, the results imply that the downflows appear when strong magnetic energy release occurs and that they are, or are correlated with, reconnection outflows.

To make the relation more clear, we plotted the correlation plot between the times of the nonthermal bursts in HXR/microwave and those of the downflows in Figure 3. The horizontal (*light gray*) and the vertical (*dark gray*) thick lines illustrate the times of the downflows and those of the nonthermal bursts, respectively. The times of the nonthermal bursts are chosen to

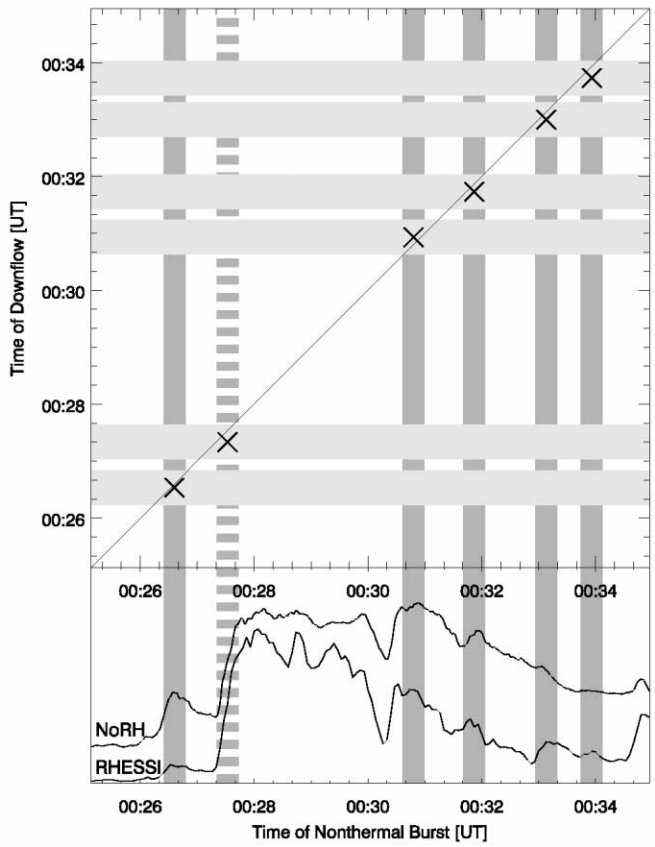

FIG. 3.—*Top*: Correlation plot between the times of the nonthermal bursts and those of the downflows. Both the horizontal and vertical axes show the times (UT). The horizontal (*light gray*) and the vertical (*dark gray*) thick lines illustrate the times of the downflows and those of the nonthermal bursts, respectively. The width of the thick lines shows the amount of error approximately. *Bottom*: Microwave (17 GHz) and HXR (50–100 keV) light curves obtained with NoRH and *RHESSI*, respectively. The thin solid line shows the points where the times of the downflows correspond to those of the HXR bursts.

be the peak times of the bursts, except for the second from the left (*dashed line*). The HXR burst, which starts at 00:27:30 UT, is the biggest, and seems to consist of some subbursts. Therefore, we chose the middle time from the start to the peak of the burst, instead of the peak time. In the bottom panel, we show the microwave (17 GHz) and HXR (50–100 keV) light curves as a comparison. The times of the downflows are selected to be the times when the downflows enter the superhot region. To determine the time, we drew a line to follow the top edge of the superhot region in the time slice images. Then, we extrapolated the path of each downflow and chose the intersection of those two lines as the time of the downflow. The thin solid line shows the points where the times of the downflows correspond to those of the HXR bursts (*diagonal line*). Only the line indicates a relationship between the two light curves. These times have fairly large errors, but nevertheless, cross points (*crosses*) of both the times lie along the diagonal line. Therefore, Figure 3 supports the suggestion that the times of the downflows correspond to the times when nonthermal bursts occur. To confirm this, we compared two time sequences of randomly occurring hypothetical features corresponding to HXR bursts and downflows and plotted them in the same way. Then, we confirmed the probability that the relationship such as indicated in Figure 3 could happen by chance is about 50%–60%. In the present case, all the downflows, at least observable ones, have their HXR burst counterparts, and the occurrence of the correlation is significantly higher than that of the random case.

4. SUMMARY AND DISCUSSION

We have examined in detail the evolution of a big two-ribbon flare that occurred on 2002 July 23. We found downflows above the postflare loops, and they are seen not only in the decay phase but also in the impulsive and main phases. Furthermore, they appear to correspond to the times when nonthermal bursts in microwaves and HXRs occurred. This result implies that the downflow motions occurred when strong magnetic energy was released and suggests that they are correlated with reconnection outflows. Thus, we have been able to add a new piece of observational evidence to the model that downflows are reconnection outflow (McKenzie & Hudson 1999; McKenzie 2000).

Another piece of observational evidence of reconnection outflows is the X-ray plasmoid ejections, which have been studied by several authors (Shibata et al. 1995; Tsuneta 1997; Ohyama & Shibata 1997, 1998). Kahler et al. (1988) reported the similar relationship between filament eruptions and HXR emissions. These observations revealed a close relationship between plasmoid ejections and HXR emissions and showed that plasmoids/filaments are strongly accelerated during the impulsive phase (i.e., during an HXR burst). A good review of the correlation between plasmoid ejections and HXR emission is presented by Aschwanden (2002). Recently, H. Takasaki (2003, private communication) found multiple X-ray plasmoid ejections, which were associated with the 2000 November 24 flare. He reported that each of the ejections appears at a time corresponding to each HXR peak in the impulsive HXR emission. Moreover, Sheeley & Wang (2002), from observations with the Large Angle Spectrometric Coronagraph aboard *SOHO*, reported that both the downflow-like features and the upward motion occur simultaneously. From these results, we suppose that both the downflows and the plasmoid ejections are reconnection outflows. We present a cartoon of this model in Figure 4. Plasmoids are generated in the current sheet, and are ejected downward (downflows) and upward (X-ray plasmoid ejections), when strong energy releases occur (Fig. 4*a*). Therefore, the correlations between plasmoid ejections, or downflow, and HXR bursts represent a plasmoid-induced, nonsteady reconnection (Shibata 1999; Shibata & Tanuma 2001). As summarized in Table 1, downflows show common features with X-ray plasmoid ejections.

What on Earth (Sun?) are the downflows? To answer this question, we have to examine the mechanism and the process of magnetic reconnection and the relationship between the reconnection outflow and the downflow in much more detail. A reconnection model and numerical simulation based on the model, which is consistent with all the features of the downflows, such as the low-density, high–Doppler shift relationship with the bursts of nonthermal emission, is required. Some authors, such as Kliem, Karlický, & Benz (2000), Tanuma et al. (2001), and so on have performed numerical simulations of magnetic reconnection and have shown that fractal plasmoids are generated in the current sheet. Kliem et al. (2000) also applied their results to the observed features in microwave emission. Those plasmoids are ejected bidirectionally, associated with the enhancement of reconnection rate. Forbes & Priest (1983), Cheng et al. (2003), and so on have studied the relationship between plasmoid ejection and enhancement of energy release in their numerical simulations. Furthermore, TanDokoro

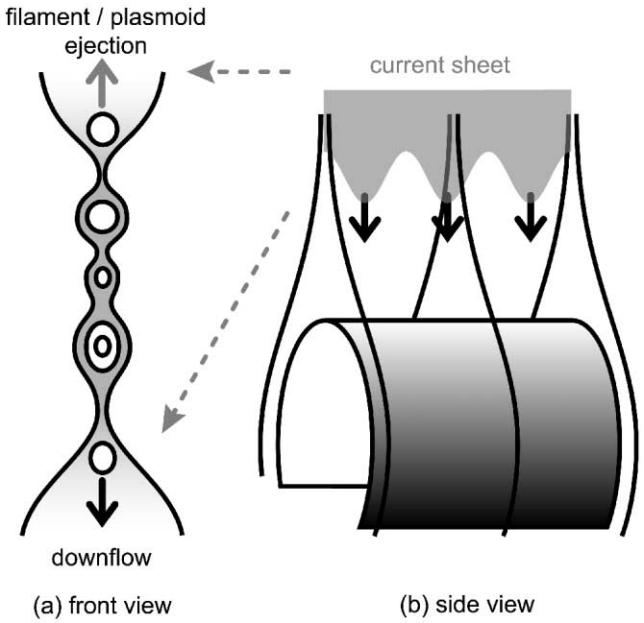

FIG. 4.—Model of the downflows and plasmoid ejections. (*a*) Front view of the structure. Many plasmoids are created inside the current sheet (*gray region*). (*b*) Side view. The current sheet is modifiied owing to some instabilities.

& Fujimoto (2004) have examined the instability at the leading edge of a reconnection jet in their new three-dimensional numerical simulation. The leading edge is modulated to be a narrow and elongated structure (as shown in the rough cartoon of Fig. 4*b*), which is similar to the shape of the downflows. These works may help to explain what downflows are.

TABLE 1

COMPARISON BETWEEN THE FEATURES OF THE PLASMOID EJECTION AND THOSE OF THE DOWNFLOW

Parameter	Plasmoid Ejection	Downflow
Velocity (km s^{-1})	30–500	45–500
Size (km)	(1–10) $\times 10^4$	(2–10) $\times 10^3$
Density (cm^{-3})	(1–10) $\times 10^9$	$\sim 10^{9a}$
Impulsive phase	Yes	Yes
Decay phase	No	Yes
HXR/microwave	Yes	Yes[b]

[a] The temperature of downflows is still uncertain.
[b] New finding in this Letter.

We first acknowledge an anonymous referee for his/her useful comments and suggestions. We wish to acknowledge all the members of Kwasan Observatory for their support during our observation, especially M. Kamobe. We again would like to thank them for their encouragement. We also thank D. H. Brooks for his careful reading and correction of this Letter. We wish to thank S. Krucker, Y. E. Litvinenko, H. S. Hudson, R. P. Lin, D. E. Innes, and V. M. Nakariakov for fruitful discussions and their helpful comments. A. A. is financially supported by a Research Fellowship from the Japan Society for the Promotion of Science for Young Scientists. We made extensive use of the *TRACE* Data Center. This work is partially supported by a Grant-in-Aid for the 21st Century COE "Center for Diversity and Universality in Physics."

REFERENCES

Akiyama, S. 2001, Ph.D. thesis, Graduate Univ. Advanced Studies
Aschwanden, M. J. 2002, Space Sci. Rev., 101, 1
Cheng, C. Z., Ren, Y., Choe, G. S., & Moon, Y.-J. 2003, ApJ, 596, 1341
Domingo, V., Fleck, B., & Poland, A. I. 1995, Sol. Phys., 162, 1
Emslie, A. G., Kontar, E. P., Krucker, S., & Lin, R. P. 2003, ApJ, 595, L107
Forbes, T. G., & Priest, E. R. 1983, Sol. Phys., 84, 169
Handy, B. N., et al. 1999, Sol. Phys., 187, 229
Hara, H., Tsuneta, S., Lemen, J. R., Acton, L. W., & McTiernan, J. M. 1992, PASJ, 44, L135
Hudson, H. S. 1991, Sol. Phys., 133, 357
Hudson, H. S., & McKenzie, D. E. 2001, Earth Planets Space, 53, 581
Hurford, G. J., Schwartz, R. A., Krucker, S., Lin, R. P., Smith, D. M., & Vilmer, N. 2003, ApJ, 595, L77
Innes, D. E., McKenzie, D. E., & Wang, T. 2003a, Sol. Phys., 217, 247
———. 2003b, Sol. Phys., 217, 267
Kahler, S. W., Moore, R. L., Kane, S. R., & Zirin, H. 1988, ApJ, 328, 824
Kliem, B., Karlický, M., & Benz, A. O. 2000, A&A, 360, 715
Krucker, S., Hurford, G. J., & Lin, R. P. 2003, ApJ, 595, L103
Lin, R. P., et al. 2002, Sol. Phys., 210, 3
———. 2003, ApJ, 595, L69
McKenzie, D. E. 2000, Sol. Phys., 195, 381
McKenzie, D. E., & Hudson, H. S. 1999, ApJ, 519, L93
———. 2001, Earth Planets Space, 53, 577
Nakajima, H., et al. 1994, Proc. IEEE, 82, 705
Neupert, W. M. 1968, ApJ, 153, L59
Ogawara, Y., Takano, T., Kato, T., Kosugi, T., Tsuneta, S., Watanabe, T., Kondo, I., & Uchida, U. 1991, Sol. Phys., 136, 1
Ohyama, M., & Shibata, K. 1997, PASJ, 49, 249
———. 1998, ApJ, 499, 934
Schrijver, C. J., et al. 1999, Sol. Phys., 187, 261
Sheeley, N. R., Jr., & Wang, Y.-M. 2002, ApJ, 579, 874
Shibata, K. 1999, Ap&SS, 264, 129
Shibata, K., Masuda, S., Shimojo, M., Hara, H., Yokoyama, T., Tsuneta, S., Kosugi, T., & Ogawara, Y. 1995, ApJ, 451, L83
Shibata, K., & Tanuma, S. 2001, Earth Planets Space, 53, 473
TanDokoro, R., & Fujimoto, M. 2004, Adv. Space Res, in press
Tanuma, S., Yokoyama, T., Kudoh, T., & Shibata, K. 2001, ApJ, 551, 312
Tsuneta, S. 1996, ApJ, 456, 840
———. 1997, ApJ, 483, 507
Tsuneta, S., et al. 1991, Sol. Phys., 136, 37
White, S. M., Krucker, S., Shibasaki, K., Yokoyama, T., Shimojo, M., & Kundu, M. R. 2003, ApJ, 595, L111
Wilhelm, K., et al. 1995, Sol. Phys., 162, 189
Wu, S. T., et al. 1986, in Energetic Phenomena on the Sun, ed. M. Kundu & B. Woodgate (NASA CP-2439; Washington, DC: NASA), 5